# Complex Representations for Learning Statistical Shape Priors

Athanasios Papaioannou
Department of Computing
Imperial College London,
U.K.

Epameinondas Antonakos
Amazon Research
Berlin
Germany

Stefanos Zafeiriou
Department of Computing
Imperial College London,
U.K.

*Abstract*—Parametrisation of the shape of deformable objects is of paramount importance in many computer vision applications. Many state-of-the-art statistical deformable models perform landmark localisation via optimising an objective function over a certain parametrisation of the object's shape. Arguably, the most popular way is by employing statistical techniques. The points of shape samples of an object lie in a 2D lattice and they are normally represented by concatenating the 2D coordinates into a vector. As the 2D coordinates can be naturally represented as a complex number, in this paper we study statistical complex number representations of an object's shape. In particular, we show that the real representation provides a similar statistical prior as the widely linear complex model, while the circular complex representation results in a much more condensed encoding.

## I. INTRODUCTION

The problem of shape representation has created a wealth of research in the fields of computer vision and pattern recognition [1], [2], [3], [4], [5]. Seminal first works included analysis of shapes via the use of non-linear morphological operators [1], [2]. In the early 2000s, the seminal shape representation for matching was the, so-called, shape context [3], which employs a histogram-based manner in order to describe the coarse arrangement of the shape with respect to a point that lies either inside or on the boundary of the shape. Recently, a very interesting method was proposed [4] that represents the shape as a non-linear surface, learned via the application of one-class Support Vector Machine (SVM), as well as a method to design rotation-invariant kernels for shape matching [5]. Additionally, state-of-the-art discriminative shape representations learned via the application of deep learning strategies [6] have been currently employed.

In this paper, we propose to learn statistical representations in the complex domain, rather than the real. This is motivated by the fact that 2D shapes can be naturally represented via the use of complex numbers. A lot of research has been recently conducted within the signal processing community towards the, so-called, Widely Linear Models (WLM) [7], [8], [9], [10]. Statistical representations in the WLM assume that the complex vector is written as a linear combination of the complex and the complex conjugate part. We show that the WLM representation provides a statistical prior space that is equivalent to the space learned via the concatenation of the real and imaginary parts of the shape (i.e., concatenation of

$x$ and $y$ coordinates). On the contrary, we show that under the assumption that the shapes are proper complex random vectors and by performing circular complex PCA, we end up with much more condensed representations.

To the best of our knowledge, the complex shape representations have only been used in order to achieve rotation invariance for the task of shape matching [5] and fitting [11]. In these works, in order to achieve rotation invariance the shape feature vectors need to be described using the complex Bingham distribution [12]. Unfortunately, there is not a known solution to estimate the normalising constant of a complex Bingham distribution, hence it is approximated by a zero-mean complex Gaussian [13].

In summary the contributions of this paper are

- We study the first, to the best of our knowledge, linear complex shape representation for the purpose of learning statistical shape priors.
- We show that the standard representation that is currently used in order to learn a statistical shape parametrisation have the same representation power as WLM.
- We show that by treating shapes as proper complex random vectors, we end up with a much more condensed statistical representation.

## II. SHAPE REPRESENTATION

A shape representation is a function that maps a number of features to a given shape. A very common way to describe a shape is by using a finite number of points, called landmarks. In the following subsections, we present how landmarks can be represented in different spaces and experimentally show the advantages and disadvantages of each representation.

### A. Real Representation

The simplest and more straightforward method to represent the $i$-th landmark of a two-dimensional shape $\mathbf{s}$ is by the vector of its Cartesian coordinates in the real plane as $\mathbf{l}_i = [x, y]^T$. The shape vector can then be retrieved by concatenating the vectors of all $n$ landmarks into a single vector as $\mathbf{s}_r = [\mathbf{l}_1^T, \ldots, \mathbf{l}_n^T]^T = [x_1, y_1, \ldots, x_n, y_n]^T$, $x_i, y_i \in \mathbb{R}$.

Thus, the shape space defined within the real domain can be denoted as $\mathbb{S} \subset \mathbb{R}^{2n}$. Note that this approach is adopted by the majority of deformable models in the computer vision literature.

### B. Complex Representation

A 2D landmark can also be naturally represented as a complex number. Kendall [14] was the first that proposed this approach. Specifically, [14] introduces the concept of "pre-shapes", which are complex vectors reformed in a suitable way in order to ensure translation, scale and rotation invariance.

In our case, we use the complex shape vectors (the "raw" landmarks [14]) instead of the "pre-shapes". By denoting a landmark in the complex space as $z_i = x_i + iy_i$, then a complex shape vector is defined as $\mathbf{s}_c = [z_1, \ldots, z_n]^T = [x_1 + iy_1, \ldots, x_n + iy_n]^T$. Consequently, it can be readily seen that this leads to an $n$-dimensional vector, thus the complex shape space is $\mathbb{C}^n$.

### C. Widely Linear Representation

A new method to better handle complex data and exploit second-order statistics was recently proposed [7]. This formulation links the real and complex representations and highlights the differences and relation between them. Furthermore, it provides a more powerful and mathematically elegant way to use complex data. In particular, instead of employing only the complex data, we also take into consideration its complex conjugate, so that the transformation depends linearly on both of them. This is the reason why it was named Widely Linear.

Given the complex shape vector $\mathbf{s}_c$ defined in Section II-B, the augmented shape vector $\underline{\mathbf{s}}$ is defined as the concatenation of the complex shape with its conjugate, i.e.

$$\underline{\mathbf{s}} \triangleq \begin{bmatrix} \mathbf{s}_c \\ \mathbf{s}_c^* \end{bmatrix} \in \mathbb{C}_*^{2n} \tag{1}$$

Let us define an augmented matrix as block matrix with a specific structure: the south-east block is the conjugate of the north-west block, and the south-west block is the conjugate of the north-east block, thus

$$\underline{\mathbf{A}} \triangleq \begin{bmatrix} \mathbf{A}_1 & \mathbf{A}_2 \\ \mathbf{A}_2^* & \mathbf{A}_1^* \end{bmatrix} \tag{2}$$

A real composite shape vector, similar to the one we defined in Section II-A, can be retrieved by concatenating the real and imaginary parts of a complex shape vector as $\tilde{\mathbf{s}} \triangleq \begin{bmatrix} \mathrm{Re}(\mathbf{s}_c) \\ \mathrm{Im}(\mathbf{s}_c) \end{bmatrix} \in \mathbb{R}^{2n}$.

The two shape spaces $\mathbb{C}_*^{2n}$ and $\mathbb{R}^{2n}$ are isomorphic. The isomorphism between them is a unitary matrix (up to a factor 2) $\mathbf{T}_n$ ($\mathbf{T}_n^H \mathbf{T}_n = \mathbf{T}_n \mathbf{T}_n^H = 2\mathbf{I}_n$) defined as

$$\mathbf{T}_n = \begin{bmatrix} \mathbf{I}_n & j\mathbf{I}_n \\ \mathbf{I}_n & -j\mathbf{I}_n \end{bmatrix} \tag{3}$$

where $\mathbf{I}_n$ is an $n \times n$ identity matrix. $\mathbf{T}_n$ can be thought as a linear map from the real data to the complex ones, namely $\underline{\mathbf{s}} = \mathbf{T}_n \tilde{\mathbf{s}} \Rightarrow \tilde{\mathbf{s}} = \frac{1}{2} \mathbf{T}_n^H \underline{\mathbf{s}}$

## III. PCA IN DIFFERENT DOMAINS

Principal Component Analysis (PCA) [15] has been used for many tasks such as dimensionality reduction and feature extraction, lossy data compression, data visualization and model construction. Furthermore, the application of PCA to acquire low-dimensional face representations initiated the development and application of CA techniques in computer vision. In the following subsections, we first present the commonly-used PCA application on real shape samples and, then, show how to construct shape models by applying PCA on different domains.

### A. Real Composite PCA

PCA was originally defined on real-valued random variables. In the case of complex data one can concatenate the real and imaginary parts and perform an eigenanalysis in the new composite real data. This approach, referred to as Real Composite PCA (RCPCA), has the advantage of avoiding the complex domain.

Specifically, as shown in Section II-C, the real composite shape vector $\tilde{\mathbf{s}}$ of $n$ landmarks lays in the $\mathbb{R}^{2n}$ domain. A training set $\mathcal{T}$ of $m$ such shape vectors can be formulated as the matrix $\tilde{\mathbf{S}} = [\tilde{\mathbf{s}}^1, \ldots, \tilde{\mathbf{s}}^m] \in \mathbb{R}^{2n \times m}$. The sample covariance matrix in $\mathbb{R}^{2n \times 2n}$ is calculated as $\mathbf{\Sigma}_r = \tilde{\mathbf{S}} \tilde{\mathbf{S}}^T$

RCPCA aims to find an orthonormal subspace $\mathbf{U}_r \in \mathbb{R}^{2n \times k}$ of $k$ components so as to maximize the variance. This optimization problem is expressed as $\mathbf{U}_r = \arg \max_{\mathbf{U}_r} \mathrm{tr}[\mathbf{U}_r^T \mathbf{\Sigma}_r \mathbf{U}_r]$, s.t. $\mathbf{U}_r^T \mathbf{U}_r = \mathbf{I}$ and the solution is given by performing eigenanalysis on the covariance matrix $\mathbf{\Sigma}_r$, i.e. $\mathbf{\Sigma}_r = \mathbf{U}_r \mathbf{\Lambda} \mathbf{U}_r^T$. Given the orthonormal basis $\mathbf{U}_r$, the mean shape $\bar{\mathbf{s}}$ and a vector of $k$ parameters (weights) $\mathbf{p} = [p_1, \ldots, p_k]$, a new shape instance can be generated using the function $S_r \in \mathbb{R}^{2n}$ defined as $S_r(\mathbf{U}_r, \bar{\mathbf{s}}, \mathbf{p}) = \bar{\mathbf{s}} + \mathbf{U}_r \mathbf{p}$.

### B. Circular PCA

Another approach is to extend directly PCA to the complex domain in a straightforward manner [7]. Instead of matrix transpose, the conjugate transpose (or Hermitian) is employed and the Hermitian covariance matrix is taken into account. Eigenanalysis is performed as usual, and real eigenvalues (because of the Hermitian covariance matrix) and complex eigenvectors are calculated. This so-called Circular Principal Component Analysis (CPCA) assumes implicitly that the data are proper and circular. A complex random signal $\mathbf{x}$ is proper if it is uncorrelated with its complex conjugate and circular iff $\mathbf{x}$ and $\mathbf{x}' = e^{i\alpha}\mathbf{x}$ have the same probability distribution for any given real $\alpha$ [16], [17]) and is optimized for circular data. However, note that in most practical applications, data are not circular and proper.

Let us assume that we have $m$ complex training shape vectors $\mathbf{S}_c = [\mathbf{s}_c^1, \ldots, \mathbf{s}_c^m]$ with $\mathbf{s}_c^i \in \mathbb{C}^n$. The sample covariance matrix in $\mathbb{C}^{n \times n}$ is $\mathbf{\Sigma}_c = \mathbf{S}_c \mathbf{S}_c^H$ In CPCA, a set of bases $\mathbf{U}_c \in \mathbb{C}^{n \times p}$ can be retrieved by solving the following maximization problem $\mathbf{U}_c = \arg \max_{\mathbf{U}_c} \mathrm{tr}[\mathbf{U}_c^H \mathbf{\Sigma}_c \mathbf{U}_c]$, s.t. $\mathbf{U}_c^H \mathbf{U}_c = \mathbf{I}$. The solution of the above optimization problem consists of the eigenvectors of the complex matrix estimated by applying eigencomposition as $\mathbf{\Sigma}_c = \mathbf{U}_c \mathbf{\Lambda}_c \mathbf{U}_c^H$.

Similar to RCPCA, given the orthonormal basis $\mathbf{U}_c$, the mean shape $\bar{\mathbf{s}}_c$ and a vector of $k$ parameters (weights) $\mathbf{p} = [p_1, \ldots, p_k]$, a function $S_c \in \mathbb{C}^n$ can be defined which generates a complex shape instance as $S_c(\mathbf{U}_c, \bar{\mathbf{s}}_c, \mathbf{p}) = \bar{\mathbf{s}}_c + \mathbf{U}_c \mathbf{p}$.

Note that, contrary to the real domain, the parameters belong in the complex domain, i.e. $p_i \in \mathbb{C}, \ \forall i = 1, \ldots, k$.

### C. Widely Linear PCA

The above complex PCA is optimal under a noise model of a circular Gaussian. That is, it employs only the information of the covariance $\mathbf{\Sigma}_c = \mathbf{S}_c \mathbf{S}_c^H$, assuming that the pseudo-covariance $\mathbf{C} = \mathbf{S}_c \mathbf{S}_c^T$ is zero. To incorporate the pseudo-covariance information we have to use the augmented complex random shapes. Widely Linear PCA (WLPCA) proposed in [7] exploits the general non-circularity of complex data. WLPCA is more general than CPCA and it has be shown that is related to its isomorphic RCPCA [8].

Using the unitary transform in Eq. 3, the augmented covariance matrix of a set of $m$ complex augmented shape vectors $[\underline{\mathbf{s}}^1, \ldots, \underline{\mathbf{s}}^m]$ can be defined as $\underline{\mathbf{\Sigma}} = \underline{\mathbf{S}}\underline{\mathbf{S}}^H = \mathbf{T}_n \mathbf{\Sigma}_r \mathbf{T}_n^H$ and the corresponding problem for the widely linear approach is to find a projection matrix $\underline{\mathbf{U}}$ such that $\underline{\mathbf{U}} = \arg\max_{\underline{\mathbf{U}}} \mathrm{tr}[\underline{\mathbf{U}}^H \underline{\mathbf{\Sigma}} \underline{\mathbf{U}}]$, s.t. $\underline{\mathbf{U}}^H \underline{\mathbf{U}} = \mathbf{I}$. In order to solve the above optimization problem we need to perform the eigenvalue decomposition to the augmented covariance matrix $\underline{\mathbf{\Sigma}}$. It has been shown [8], [18] that the eigenvalues and eigenvectors of the augmented matrix are related with the respective eigenvalues and eigenvectors of the real covariance matrix $\mathbf{\Sigma}_r$ as $\underline{\mathbf{U}} = \mathbf{T}_n \mathbf{U}_r \mathbf{T}_{\frac{H}{2}}$.

Given an augmented subspace $\underline{\mathbf{U}}$, the corresponding mean shape $\bar{\underline{\mathbf{s}}}$ and a set of parameters $\underline{\mathbf{p}} = [\mathbf{p}^T, \mathbf{p}^H]^T$, a new shape instance can be generated using the function

$$S(\underline{\mathbf{U}}, \bar{\underline{\mathbf{s}}}, \underline{\mathbf{p}}) = \bar{\underline{\mathbf{s}}} + \underline{\mathbf{U}}\underline{\mathbf{p}} \Rightarrow S(\underline{\mathbf{U}}, \bar{\underline{\mathbf{s}}}, \underline{\mathbf{p}}) = \bar{\mathbf{s}} + \mathbf{U}_1 \mathbf{p} + \mathbf{U}_2 \mathbf{p}^* \quad (4)$$

where $\mathbf{U}_1$ and $\mathbf{U}_2$ are defined using the augmented matrix structure of Eq. 2.

## IV. EXPERIMENTS

In this section we present a comprehensive comparison of the performance of the different shape representations. We evaluate the reconstruction power of each shape representation for three different deformable objects, i.e. human body and hands (articulated objects) as well as human face (non-articulated object).

**Databases** We use the 68 points annotations provided by [19], [20] for the well-known HELEN [21] (2000 images) and LFPW [22] (811 images). All the images are collected from Flickr and are captured under "in-the-wild" conditions, hence they include a large variance of head poses and expressions. We randomly separated the total of 2811 shapes into 2000 and 811 that were used for training and testing, respectively.

For the case of human body, we employ the Fashion-Pose [23] dataset which is one of the few available databases that include images captured in totally unconstrained conditions. It is a recently collected dataset that contains 7543 annotated images which were acquired from online fashion blogs. Each image contains a person where the full body is visible and is annotated by 13 landmarks even in the images where occlusions have occurred. Both the large variation of dressing style and pose increase the difficulty of the dataset.

Originally, the training set contained 6543 images and the testing set 1000 images. In our experiments, we keep the same size for both of them.

Finally, in the case of human hand, we use our in-house dataset which includes 1200 images that are manually annotated with 39 points. We collected the data from Google Images, trying to acquire as much variability as possible. For the purpose of our experiments, we split the dataset into two sets of 1000 and 200 shapes that are used for training and testing, respectively.

**Results** The evaluation of the employed shape representations is based on the reconstruction error [24], [25]. The reconstruction of a shape vector $\mathbf{s}$ in all domains can be retrieved using the generalized equation $\mathbf{s}_r = \bar{\mathbf{s}} + \mathbf{U}\mathbf{U}^H(\mathbf{s} - \bar{\mathbf{s}})$, where $\mathbf{U}$ denotes the basis and $\bar{\mathbf{s}}$ is the mean shape vector. Of course, $\mathbf{U}$ and $\bar{\mathbf{s}}$ need to be replaced by the corresponding bases and mean vectors of each domain. Given a matrix of $m$ testing shape vectors $\mathbf{S}$ and their reconstructions $\mathbf{S}_r$, the reconstruction error is computed as $e_r = \frac{1}{m} \|\mathbf{S} - \mathbf{S}_r\|_F^2$.

Figure 1 shows the reconstruction error for all the shape representations in the three different datasets. Complex circular representation outperforms the other two in all the datasets even though the widely linear and the real model are considered to be more general. This leads us to the conclusion that the complex circular is more robust and more condensed than the other two representations as it needs much fewer components to succeed better results.

Figures 2, 3 and 4 demonstrate indicative shapes generated by the real, complex and widely linear models, respectively. Specifically, the central shape of each figure shows the mean shape of the object. The shapes on the top and bottom of the mean shape are synthesised using the first eigenvector (the shape on the top is produced with a positive weight and the one on the bottom with a negative). The shapes on the right and left are generated from the second eigenvector. Finally, the shapes on the main and secondary diagonals are synthesized using the third and fourth components, respectively.

As it can be seen, the complex shape model is able to include more information than the other two representations. Widely linear and real representations have similar behaviour. However, the complex eigenvectors are more condensed. For example, in the case of face, the first eigenvector incorporates both the horizontal (yaw) and vertical (pitch) pose, while the real and widely linear representations require two components to express the same deformations. This can be a valuable advantage within the optimization procedure of a statistical deformable model (e.g. Active Appearance Model, Constrained Local Model), since the search space of the cost function is more compact.

## V. CONCLUSION

In this paper we examined how to represent shape in different ways and particularly in the complex domain. We explained how to perform widely linear PCA and complex PCA and what are the differences between them. Additionally, we showed that the standard representation that is currently
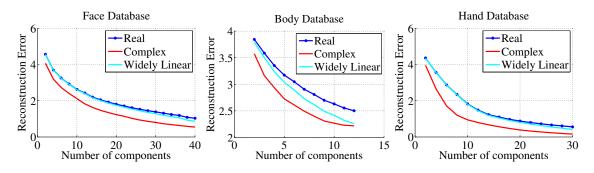
Fig. 1. Reconstruction experiments on face (*left*), body (*center*) and hand (*right*) databases using the three shape representations.
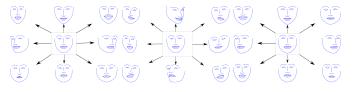


Fig. 2. The mean shape and shape instances generated from the first four eigenvectors for the real(*left*), complex(*center*) and widely linear(*right*) shape representations for human face.
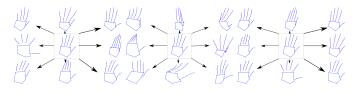


Fig. 3. The mean shape and shape instances generated from the first four eigenvectors for the real(*left*), complex(*center*) and widely linear(*right*) shape representations for human hand.
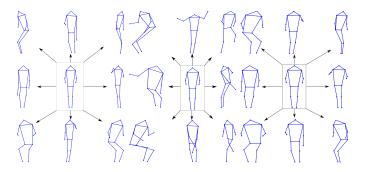


Fig. 4. The mean shape and shape instances generated from the first four eigenvectors for the real(*left*), complex(*center*) and widely linear(*right*) shape representations for human body.

used in order to learn a statistical shape parametrisation has the same representation power as the widely linear model. Finally, we examined the reconstruction and representation power of each model on three different articulated and non-articulated objects through quantitative and qualitative experimental results.

## VI. Acknowledgements

## References

[1] Petros Maragos, "Pattern spectrum and multiscale shape representation," *Pattern Analysis and Machine Intelligence, IEEE Transactions on*, vol. 11, no. 7, pp. 701–716, 1989.

[2] Ioannis Pitas and Anastasios N. Venetsanopoulos, "Morphological shape decomposition," *IEEE Transactions on Pattern Analysis & Machine Intelligence*, , no. 1, pp. 38–45, 1990.

[3] Serge Belongie, Jitendra Malik, and Jan Puzicha, "Shape matching and object recognition using shape contexts," *Pattern Analysis and Machine Intelligence, IEEE Transactions on*, vol. 24, no. 4, pp. 509–522, 2002.

[4] Hien Van Nguyen and Fatih Porikli, "Support vector shape: A classifier-based shape representation," *Pattern Analysis and Machine Intelligence, IEEE Transactions on*, vol. 35, no. 4, pp. 970–982, 2013.

[5] O.C. Hamsici and A.M. Martinez, "Rotation invariant kernels and their application to shape analysis," *Pattern Analysis and Machine Intelligence, IEEE Transactions on*, vol. 31, no. 11, pp. 1985–1999, Nov 2009.

[6] Qian Yu, Yongxin Yang, Yi-Zhe Song, Tao Xiang, and Timothy M Hospedales, "Sketch-a-net that beats humans," in *Proceedings of the British Machine Vision Conference (BMVC)*, 2015, pp. 7–1.

[7] P.J. Schreier and L.L. Scharf, "Second-order analysis of improper complex random vectors and processes," *IEEE T-SP*, vol. 51, no. 3, pp. 714–725, 2003.

[8] A. Papaioannou and S. Zafeiriou, "Principal component analysis with complex kernel: The widely linear model," *Neural Networks and Learning Systems, IEEE Transactions on*, vol. 25, no. 9, pp. 1719–1726, Sept 2014.

[9] Pantelis Bouboulis and Sergios Theodoridis, "Extension of wirtinger's calculus to reproducing kernel hilbert spaces and the complex kernel lms," *IEEE Transactions on Signal Processing*, vol. 59, no. 3, pp. 964–978, 2011.

[10] Pantelis Bouboulis, Konstantinos Slavakis, and Sergios Theodoridis, "Adaptive learning in complex reproducing kernel hilbert spaces employing wirtinger's subgradients," *Neural Networks and Learning Systems, IEEE Transactions on*, vol. 2, no. 99, pp. 260–276, 2012.

[11] Onur C Hamsici and Aleix M Martinez, "Active appearance models with rotation invariant kernels," in *Computer Vision, 2009 IEEE 12th International Conference on*. IEEE, 2009, pp. 1003–1009.

[12] Ian L Dryden and Kanti V Mardia, *Statistical shape analysis*, vol. 4, Wiley Chichester, 1998.

[13] Onur C Hamsici and Aleix M Martinez, "Spherical-homoscedastic distributions: The equivalency of spherical and normal distributions in classification.," *Journal of Machine Learning Research*, vol. 8, no. 1583-1623, pp. 1–3, 2007.

[14] David G Kendall, "Shape manifolds, procrustean metrics, and complex projective spaces," *Bulletin of the London Mathematical Society*, vol. 16, no. 2, pp. 81–121, 1984.

[15] T. Jollife, "Principal component analysis," *Berlin: Springer*, pp. 559–572, 2002.

[16] T. Adali, P.J. Schreier, and L.L. Scharf, "Complex-valued signal processing: The proper way to deal with impropriety," *IEEE T-SP*, vol. 59, no. 11, pp. 5101–5125, 2011.

[17] Danilo Mandic and Vanessa Su Lee Goh, *Complex Valued Nonlinear Adaptive Filters: Noncircularity, Widely Linear and Neural Models*, Wiley Publishing, 2009.

[18] P.J. Schreier and L.L. Scharf, *Statistical Signal Processing of Complex-Valued Data: The Theory of Improper and Noncircular Signals*, Cambridge University Press, Cambridge, UK, 2010.

[19] Christos Sagonas, Georgios Tzimiropoulos, Stefanos Zafeiriou, and Maja Pantic, "300 faces in-the-wild challenge: The first facial landmark localization challenge," in *Computer Vision Workshops (ICCVW), 2013 IEEE International Conference on*. IEEE, 2013, pp. 397–403.

[20] Christos Sagonas, Georgios Tzimiropoulos, Stefanos Zafeiriou, and Maja Pantic, "A semi-automatic methodology for facial landmark annotation," in *Computer Vision and Pattern Recognition Workshops (CVPRW), 2013 IEEE Conference on*. IEEE, 2013, pp. 896–903.

[21] Vuong Le, Jonathan Brandt, Zhe Lin, Lubomir Bourdev, and Thomas S Huang, "Interactive facial feature localization," in *Computer Vision–ECCV 2012*, pp. 679–692. Springer, 2012.

[22] Peter N Belhumeur, David W Jacobs, David J Kriegman, and Narendra Kumar, "Localizing parts of faces using a consensus of exemplars," *Pattern Analysis and Machine Intelligence, IEEE Transactions on*, vol. 35, no. 12, pp. 2930–2940, 2013.

[23] M. Dantone, J. Gall, C. Leistner, and L. Van Gool, "Human pose estimation using body parts dependent joint regressors," in *Computer Vision and Pattern Recognition (CVPR), 2013 IEEE Conference on*, June 2013, pp. 3041–3048.

[24] Chris Ding, Ding Zhou, Xiaofeng He, and Hongyuan Zha, "R1-pca: Rotational invariant l1-norm principal component analysis for robust subspace factorization," *ACM*, pp. 281–288, 2006.

[25] Nojun Kwak, "Principal component analysis based on l1-norm maximization," *IEEE T-PAMI*, vol. 30, no. 9, pp. 1672–1680, 2008.